Published in final edited form as:
J Proteomics. 2013 March 27; 80: . doi:10.1016/j.jprot.2013.01.013.

Network of brain protein level changes in glutaminase deficient fetal mice

Narkhyun Bae[1], **Yvonne Wang**[2], **Lin Li**[1], **Stephen Rayport**[2,3,*], and **Gert Lubec**[1,*]

[1]Department of Pediatrics, Medical University of Vienna, Währinger Gürtel 18, 1090 Vienna, Austria

[2]Department of Psychiatry, Columbia University, 1051 Riverside Drive, NYPSI Unit 62, New York, NY 10032, USA

[3]Division of Molecular Therapeutics, New York State Psychiatric Institute, 1051 Riverside Drive, NYPSI Unit 62, New York, NY 10032, USA

Abstract

Glutaminase is a multifunctional enzyme encoded by gene Gls involved in energy metabolism, ammonia trafficking and regeneration of neurotransmitter glutamate. To address the proteomic basis for the neurophenotypes of glutaminase-deficient mice, brain proteins from late gestation wild type, Gls+/- and Gls-/- male mice were subjected to two-dimensional gel electrophoresis, with subsequent identification by mass spectrometry using nano-LC-ESI-MS/MS. Protein spots that showed differential genotypic variation were quantified by immunoblotting. Differentially expressed proteins unambiguously identified by MS/MS included neurocalcin delta, retinol binding protein-1, reticulocalbin-3, cytoskeleton proteins fascin and tropomyosin alpha-4-chain, dihydropyrimidinase-related protein-5, apolipoprotein IV and proteins from protein metabolism proteasome subunits alpha type 2, type 7, heterogeneous nuclear ribonucleoprotein C1/C2 and H, voltage-gated anion-selective channel protein 1 and 2, ATP synthase subunit ß and transitional endoplasmic reticulum ATPase. An interaction network determined by Ingenuity Pathway Analysis revealed a link between glutaminase and calcium, Akt and retinol signaling, cytoskeletal elements, ATPases, ion channels, protein synthesis and the proteasome system, intermediary, nucleic acid and lipid metabolism, huntingtin, guidance cues, transforming growth factor beta-1 and hepatocyte nuclear factor 4-alpha. The network identified involves (a) cellular assembly and organization and (b) cell signaling and cell cycle, suggesting that Gls is crucial for neuronal maturation.

Keywords

Glutaminase; Gls; Schizophrenia; Protein network; LC-MS/MS

[*]To whom correspondence should be addressed: Gert Lubec, Professor, FRSC (UK), Medical University of Vienna, Dept. of Pediatrics, Währinger Gürtel 18, A 1090 Vienna, Austria; +43-1-40400-3215; gert.lubec@meduniwien.ac.at; Stephen Rayport, MD PhD, Columbia University, Dept. of Psychiatry; 1051 Riverside Drive, NYPSI Unit 62, New York, NY 10032, USA; +1-212-543-5641; sgr1@columbia.edu.

Introduction

In the brain, the kidney-type glutaminase (KGA; EC 3.5.1.2) is a crucial neuronal enzyme that deamidates glutamine (Gln) to stoichiometric amounts of glutamate (Glu) and ammonia [1,2]. KGA is a heterotetrameric enzyme consisting of three 66 kDa subunits and one 68 kDa subunit in the inner membrane of mitochondria [3,4]. The catalytic rate of KGA is regulated by neuronal activity, dependent on phosphate for activation, and is strongly inhibited by its reaction products, Glu and ammonia. The predominant form of glutaminase in the brain is type 1 or brain-kidney type which is encoded by GLS on human chromosome 2q32-q34 [5,6] and mouse chromosome 1. Type 2 or liver-type glutaminase (LGA), which is encoded by GLS2 on human chromosome 12q13 and mouse chromosome 10, contributes only a small minority of glutaminase activity; it is found in nuclei suggesting a non-neurotransmitter role [7,8].

Glu is the predominant excitatory neurotransmitter in mammalian brain, a major source of cell energy, the precursor of γ-aminobutyric acid (GABA), and glutathione. After release into the synaptic cleft, Glu is taken up by adjacent astrocytes and converted to Gln by glutamine synthase. The majority of neurotransmitter Glu is recycled through this Gln-Glu shuttle between neurons and astrocytes [9-11]. While there has been a general acceptance of the Gln-Glu cycle as a major source of neurotransmitter glutamate [12], more recent findings have questioned this [13,14]. Indeed, three Gln-independent cycles for Glu trafficking involving tricarboxylic acid cycle intermediates have been identified [15].

Mice with heterozygous reductions in Gls show similar reductions in KGA [16] and elevations in Gln (the glutaminase substrate), and a global reduction in Glu/Gln ratios, showing that genetic compromise of Gls yields a neurochemical phenotype likely to impact Glu neurotransmission [17]. Both spontaneous and evoked synaptic input are reduced in the hippocampus, but not in the anterior cingulate cortex. This regional difference is consistent with the heterogeneity of systems that maintain Glu synaptic homeostasis, including neuronal Glu re-uptake [18] and anapleurosis from Gln via the tricarboxylic acid cycle [15].

Altered Gluergic neurotransmission is central to a wide range of neuropsychiatric conditions. High concentrations of extracellular Glu lead to excitotoxicity, neuronal damage by prolonged activation of Glu receptors in stroke and a range of other neurodegenerative disorders [19-21]. Release of KGA from dying neurons can extend the excitotoxic cascade, which has suggested that KGA inhibitors may reduce stroke size [22]. Alterations in the cortical Gluergic and GABAergic signal transduction are involved in depression [23] and increased KGA expression and activity has been found in postmortem brains of patients with schizophrenia (SCZ) [24,25], consistent with the dysregulation of Gluergic neurotransmission recognized in SCZ [26].

Gls null mice (Gls-/-) die shortly after birth [16]. Prior to their demise, Gls null mice show disorganized behavior, making it impossible for them to suckle, and they fail to ingest milk; however, dropper feeding them milk does not avert their demise. Thus, they appear to have a broader deficit in glutamatergic synaptic transmission accounting for their inability to coordinate their behavior. In Gls null neuronal cultures, baseline excitatory synaptic activity is unaffected while evoked excitatory synaptic responses are exhausted more rapidly. While other pathways produce sufficient Glu for baseline Gluergic transmission [15], Gls appears to be essential for maintaining the normal function of active synapses. Thus, Gluergic synapses lacking KGA show an activity-dependent deficit, presumably accounting for altered rhythmic neuronal activity affecting both breathing and coordinated motor behavior.

Consistent with the role of Gln as a major energy source [5], Gls-/- mice are born about 10% smaller than their wild type (WT) littermates [16], suggesting that they are at a metabolic

disadvantage. In contrast, Gls heterozygous (het) mice (Gls+/-) are normal sized and display neither behavioral abnormalities nor SCZ-associated phenotypes; rather, the mice show a SCZ resilient phenotype [17]. Gls hets show diminished amphetamine-induced behavioral stimulation and striatal dopamine release, two animal correlates of positive symptoms in schizophrenia (SCZ). In contrast to patients with SCZ, Gls hets showed diminished ketamine-induced frontal cortex activation. They show enhanced latent inhibition, a behavioral measure typically diminished in SCZ and enhanced by antipsychotic drugs. Most strikingly, the mice show a focal hippocampal hypoactivity on brain imaging that is the inverse of the hyperactivity seen in patients with SCZ [27].

These results raise the question as to whether the SCZ resilient phenotype arises because of the constitutive reduction in KGA expression throughout life or reduced KGA activity in adulthood. More broadly, many transgenic studies assume that heterozygous mice do not differ from WT mice because of functional reserve. To address these issues, we examined the molecular consequences of Gls knockdown and knockout at the proteomic level during fetal development. This revealed a network of KGA-dependent proteins and their interaction partners that showed differential genotypic variation.

Material and methods

Animals

Procedures involving mice and their care were performed under protocols approved by the Institutional Animal Care and Use Committees of Columbia University and New York State Psychiatric Institute, following the guidelines of the National Institutes of Health *Guide for the Care and Use of Laboratory Animals*. Gls het (Gls+/-) mice with one copy of a floxed PGK*neo*-Stop cassette (stopGls allele) inserted ahead of the transcription initiation site in exon 1 of the *Gls* gene (Entrez Gene 14660) were kept on a 129SvEv/J background [16] and bred to yield WT (Gls+/+), heterozygous (Gls+/-) and null (Gls-/-) fetuses. At about 17 – 21 days gestation, dams were anesthetized with ketamine/xylazine and fetuses harvested to ice chips. Brains were rapidly extracted, flash frozen by immersion in isopentane on dry ice, and stored at -80 °C until analysis. Tail samples were sent to Transnetyx (Cordova, TN, USA) for automated genotyping for Gls WT and stopGls alleles and a y-chromosome maker for sex determination. A total of 10 dams, dissected on 7 separate dates spanning 8 months, provided the 30 male fetuses used.

Sample preparation for Two-Dimensional gel Electrophoresis (2DE)

Whole brains were homogenized and suspended in 1.2mL sample buffer (20mM Tris, 7M urea, 2M thiourea, 4% w/v CHAPS, 10mM 1,4-dithioerythritol, 1mM EDTA, 1mM PMSF, 1 tablet Complete™ from Roche Diagnostics (Graz, Austria), and 0.2% v/v phosphatase inhibitor cocktail from Calbiochem (Darmstadt, Germany). The suspension was sonicated on ice for approximately 30 s and centrifuged at 15,000 × g for 120 min at 4°C. Desalting was carried out with an Ultrafree-4 centrifugal filter unit with a cut off molecular weight of 10 kDa (Millipore, Wien, Austria) at 3000 × g at 4°C until the eluted volume was about 4mL and the remaining volume reached 100–200 μL. The protein content of the supernatant was determined by the Bradford assay.

2DE

Samples of 700μg protein were subjected to immobilized pH 3–10 nonlinear gradient strips. Focusing started at 200 V and the voltage was gradually increased to 8000 V at 4 V/min and kept constant for a further 3 h (approximately, 150 000 Vh totally). Prior to the second dimensional run, strips were equilibrated twice for 15 min with gentle shaking in 10mL of SDS equilibration buffer (50mM pH 8.8 Tris-HCl, 6M urea, 30% v/v glycerol, 2% w/v SDS,

trace of bromophenol blue). DTT (1% w/v) was added at the first incubation for 15 min and 4 % iodoacetamide w/v instead of DTT at the second incubation step for 15 min. The second dimensional separation was performed on 10–16% gradient SDS-PAGE. After protein fixation for 12 h in 50% methanol and 10% acetic acid, gels were stained with colloidal Coomassie blue (Novex, San Diego, CA, USA) for 8 h and excess of dye was washed out from the gels with distilled water. Molecular masses were determined by running precision protein standard markers (Bio-Rad Laboratories Technologies, Hercules, CA, USA), covering the range of 10–250 kDa. pI values were determined as given by the supplier of the immobilized pH gradient strips.

Quantification of protein levels

Protein spots from each gel were outlined (first automatically and then manually) and quantified using the PDQuest 2-D analysis software (Bio-Rad). The percentage of the volume of the spots representing a certain protein was determined in comparison with the total proteins present in the 2-DE gel. The software used also revealed that spots evaluated did not contain other proteins. Moreover, only well-separated spots were considered for quantification. Only those proteins (spots) with significantly different genotypic levels were identified.

Analysis of peptides by nano-LC-ESI-(CID/ETD)-MS/MS (high capacity ion trap)

Proteins in spots that showed genotypic differences were manually excised and placed into 1.5-mL lobind Eppendorf tubes. Gel plugs were washed with 10mM ammonium bicarbonate and 50% ACN in 10mM ammonium bicarbonate repeatedly. Addition of 100% ACN resulted in gel shrinking and the shrunk gel plugs were then dried in a Speedvac Concentrator 5301 (Eppendorf, Germany). The dried gel pieces were reswollen and in-gel digested with 40 ng/mL trypsin (Promega, Madison, WI, USA) in digestion buffer, consisting of 5mM octyl β-D-glucopyranoside (OGP) and 10mM ammonium bicarbonate, and incubated over night at 37 °C. Chymotrypsin (Roche-Diagnostics) digestion was done in 25mM NH_4HCO_3, 5mM OGP and kept at 30°C for 2 h. After MS analysis of trypsin-digested proteins, proteins of low sequence coverage (below 30%) were selected for chymotrypsin digestion. Peptide extraction was performed with 10 mL of 10mM ammonium bicarbonate overnight, 15 mL of 1% formic acid (FA) in 5mM OGP for 30min, 15 mL of 0.1% FA for 30min, and subsequently 0.1% FA in 20% ACN for 30min. The extracted peptides were pooled for high-capacity ion trap (HCT) analysis.

In total, 40 μL of extracted peptides was analyzed by HCT. The HPLC used was a bio-compatible Ultimate 3000 system (Dionex, Sunnyvale, CA, USA) equipped with a PepMap100 C-18 trap column (300 mm × 5mm) and PepMap100 C-18 analytic column (75 -150 mm). The gradient was (A: 0.1% FA in water, B: 0.08% FA in ACN) 4–30% B from 0 to 105 min, 80% B from 105 to 110 min, 4%B from 110 to 125 min. The flow rate was 300 nL/min from 0 to 12 min, 75 nL/min from 12 to 105 min, and 300 nL/min from 105 to 125 min. A HCT ultra PTM discovery system (Bruker Daltonics, Bremen, Gemany) was used to record peptide spectra over the mass range of m/z 350–1500, and MS/MS spectra in information-dependent data acquisition over the mass range of m/z 100–2800. Repeatedly, MS spectra were recorded followed by three data-dependent CID MS/MS spectra and three ETD MS/MS spectra generated from three highest intensity precursor ions. An active exclusion of 0.4 min after two spectra was used to detect low abundant peptides. The voltage between ion spray tip and spray shield was set to 1100 V. Drying nitrogen gas was heated to 170° C and the flow rate was 10 L/min. The collision energy was set automatically according to the mass and charge state of the peptides chosen for fragmentation.

Multiple-charged peptides were chosen for MS/MS experiments base on their good fragmentation characteristics. MS/MS spectra were interpreted and peak lists were generated by DataAnalysis 3.4 (Bruker Daltonics). Searches were done by using MASCOT 2.2.04 (Matrix Science London, UK) against the latest UniProtKB (http://www.uniprot.org) for protein identification. Searching parameters were set as follows: enzyme selected as trypsin or chymotrypsin with two maximum missing cleavage sites, species limited to mouse, a mass tolerance of 0.2 Da for peptide tolerance, 0.2 Da for MS/MS tolerance, fixed modification of carbamidomethyl (C), and variable modification of methionine oxidation and phosphorylation (Tyr, Thr, and Ser). Positive protein identifications were based on a significant MOWSE score. After protein identification, an error-tolerant search was done to detect nonspecific cleavage and unassigned modifications. Protein identification and modification information returned from MASCOT were manually inspected and filtered to obtain confirmed protein identification and modification lists of CID MS/MS and ETD MS/MS.

Western blotting

In order to verify the results obtained from 2-DE quantification of identified proteins, 10∼20 μg of protein samples each were loaded onto 10% SDS homogenous gels, followed by electrophoresis with the Criterion cell 1D electrophoresis system (Bio-Rad Laboratories). Proteins separated on the gels were transferred onto PVDF membranes (Millipore). After blocking with 5% non-fat dry milk in 0.1% TBST, membranes were incubated with the antibodies listed in Table 1. Primary antibodies were detected with horseradish peroxidase-coupled anti-goat (Santa Cruz Biotechnology, Santa Cruz, CA, USA; #A2508) anti-rabbit IgG and anti-mouse IgG (Cell Signaling Technologies, Danvers, MA, USA; #7076) according to the supplier's protocol. Membranes were developed with the Pierce ECL Western Blotting Substrate (Thermo Fisher Scientific, Rockford, IL, USA). Densities of immunoreactive bands were measured using *Image J* (http://rsb.info.nih.gov/ij/).

Pathway analysis

Differentially expressed proteins were analyzed further by bioinformatic pathways analysis (Ingenuity Pathway Analysis [IPA]; Ingenuity Systems, Mountain View, CA; www.ingenuity.com). IPA constructs hypothetical protein interaction clusters on the basis of a regularly updated *Ingenuity Pathways Knowledge Base* [28-30].

Statistical analysis

Statistical analysis to reveal between-group differences in protein expression was performed using one-way ANOVA followed by a *post hoc* test where appropriate, with significance set at $P < 0.05$. All calculations including Bonferroni's test for multiple comparisons were performed using GraphPad Prism software (GraphPad Software, La Jolla, CA92037, USA) and SPSS 14.0 (SPSS, Chicago, IL, USA).

Results

The brains of late gestation male mouse fetuses of Gls WT, heterozygous, and null genotypes (n=10 of each genotype) were extracted. As shown previously [16], immunoblotting confirmed genotypic reductions in KGA, with greater than a 50% reduction in Gls het and no detectable KGA in Gls null brain (Figure 1).

Whole brain proteins were separated on 2DE gels. Proteins showing genotypic variation were identified and are shown labeled by their UniProtKB accession numbers for each genotype (Figure 2). In total, 33 spots representing 32 proteins showed statistically different brain levels between the three genotypes (Table 2 and supplemental figure 1). Identification

results are provided in Supplemental Table 1, listing spot numbers, UniProtKB accession numbers, sequence coverages, MS/MS peptide sequences, mass errors, ion scores and the enzyme used for in-gel digestion. Lowest sequence coverage observed was 30% and proteins were unambiguously identified according to published identification criteria [31].

Protein quantification of 2DE gel spots showed that 13 proteins were significantly altered in both Gls het and null brain (Table 2, group 3). These proteins included neurocalcin-delta (Spot 6), proteasome subunit alpha type 2 (Spot 92), and beta type 2 (Spot 93), Proteasome subunit alpha type-7 (Spot 108), voltage-dependent anion selective channel protein 1 and 2 (Spot 116 (1) and (2)), cytosolic 5`nucleotidase III-like protein (Spot 35), reticulocalbin 3 (Spot 175), apolipoprotein A4 (Spot 181), heterogeneous ribonucleoprotein D-like (Spot 194), acety-CoA-acetyltransferase (Spot 224), fascin (Spot 354) and dihydrolipoyl dehydrogenase (Spot 359).

There were 9 proteins that were altered in Gls het but not Gls null brain (Table 2, group 1). These were retinol binding protein 1 (Spot 19), S-methyl-5`thioadenosine phosphorylase (Spot 109), STIP1 homology and Ubox-containing protein 1 (Spot 156), elongation factor Tu (Spot 234), tubulin beta 2B (Spot 282) and 4 chain (Spot 287), ATP synthase subunit beta (Spot 288), lamin B1 (Spot 302), dihydropyrimidinase-related protein 5 (Spot 373).

There were 10 proteins that were only altered in Gls null brain (Table 2, group 2). These were triose phosphate isomerase (represented by two expression forms; Spots 98 and 102), protein ADP-ribosylarginine hydrolase (Spot 149), heterogeneous nuclear ribonucleoproteins C1/C2 (Spot 171), alpha-2-macroglobulin receptor-associated protein (Spot 225), 26S protease regulatory subunit 10B (Spot 226), dihydropyrimidinase related protein 3 (Spot 334), heterogenous nuclear ribonucleoprotein H (Spot 350), bifunctional purine biosynthesis protein PURH (Spot 370) and transitional endoplasmic reticulum ATPase (Spot 292). Tropomyosin alpha 4 chain was only significantly different het vs. null (Table 2, group 4) and so was not included in the pathway analysis.

Proteins showing the largest change included ATP synthase subunit beta (Spot 288), which was over 8 fold increased in hets, and Bifunctional purine biosynthesis protein PURH (Spot 370), which was reduced 4 fold in nulls. The most abundant protein showing significant genotypic alteration was Tubulin beta-2B chain (Spot 282), which showed identical genotypic reductions in hets and Nulls.

Results from 2DE were largely confirmed on western blotting (Figure 3). Gel-based proteomics results were confirmed for the neurocalcin-delta, retinol binding protein 1, proteasome subunit alpha types 2 and 7, reticulocalbin 3, heterogeneous nuclear ribonucleoproteins C1/C2 and H, tropomyosin alpha 4 chain, dihydropyrimidinase-related protein 5, fascin, apolipoprotein A-4, voltage-dependent anion-selective channel proteins 1 and 2, ATP synthase subunit beta, transitional reticulum ATPase and beta-actin was used as loading control.

Network pathway analysis integrated the majority of proteins identified as changed on 2DE (Table 2), as shown in Figure 4 but did not include S-methyl-5`thioadenosine phosphorylase, and lamin B1 because of low scoring. Reticulocalbin 3 was not identified as a network component in the analysis, but is closely coupled to calcium signaling pathways [32] in the network. The individual links between proteins are provided and referenced in supplemental Table 2.

Significant correlations between transitional reticulum ATPase and ATP synthase subunit beta as well as between proteasomal subunit alpha type 2 and 7 were observed (Supplemental Figure 2), complementing the network established by IPA networking.

Discussion

Genotypic reduction in KGA drives a network linking a series of individual pathways indicating the far reaching effect of the Gls knockdown or knockout on signaling, metabolic, cytoskeleton, guidance cues, protein synthetic and degradation cascades as well as ion channels. And this is in line with previous work suggesting a series of metabolic functions for glutaminases [7,8,33,34,35,36,37,38]. Most affected proteins showed progressive genotypic variation, while a few were unaffected in hets and only affected in nulls. Levels of neurocalcin-delta, retinol binding protein 1, heterogeneous ribonucleoprotein C1/C2, tropomyosin alpha4, apolipoprotein IV, voltage-dependent anion-selective channel protein 1 and transitional endoplasmic reticulum ATPase were dramatically changed probably suggesting biological effects. The findings may propose changes in glutamatergic neurotransmission probably shifting the equilibrium between glutamine/glutamate that may well lead to neuropsychological changes observed in adult Gls hets [39,40]. In addition, changes of the voltage-dependent anion-selective channel proteins may suggest alterations of neural transmission as observed in human neurodegenerative disorders [41]. Wiring of the brain depends on guidance cues and collapsins including dihydropyrimidinase-related proteins and indeed, protein level changes of dihydropyrimidinase-related proteins 3 and 5 were observed in Gls hets and null mice. These findings prompt the evaluation of Gls deficient mice for morphological and functional changes indicative of abnormal brain wiring.

Network analyses indicate that huntingtin is linked to a series of the proteins STIP-1 homology and U box containing protein 1 (STUB1), triose phosphate isomerase 1 (TPI-1), dihydrolipoyl dehydrogenase (DLD), heterogeneous ribonucleoprotein C1/C2, ATP synthase subunit beta and voltage-dependent anion-selective channel protein 2 (VDAC2). VDAC2 directly interacts with huntingtin protein (HTT) and it is has been suggested that huntingtin-interacting proteins are genetic modifiers of neurodegeneration [42] and huntingtin is known to play a role for translational events modifying protein synthesis *per se* [43]. It remains open if the neurological and neuropathological changes observed in the Gls hets resemble or involve elements of Huntington's disease. The inclusion of Akt as a major signaling cascade in the brain additionally serves to suggest neurological and psychomotor changes in hets. The serine/threonine protein kinase Akt controls synaptic strength [44,45], synaptic scaling [46], synapse and dendritic spine formation [47], synaptic plasticity [48], neurogenesis [49], dopaminergic neurotransmission and behavior [50] as well as metabotropic glutamate receptor-dependent long-term depression [51]. Based on the proposed network analysis, studying the Akt pathway in Gls hets with the reported neuropsychiatric phenotype appears mandatory.

KGA has multiple functions. Its genotypic reduction is associated with changed enzyme levels in several metabolic pathways involving carbohydrate, intermediary energy and lipid metabolism, protein synthesis and degradation, splicing, and purine and nucleic acid metabolism. Thus its genotypic reduction is associated with complex molecular changes in the brains of Gls hets and null mice. This multiple metabolic impacts may also account for their observed reduced size and body weight of the Gls nulls [16].

Possible involvement of calcium signaling in the brain is indicated by the links between calcium, glutaminase [39], tubulin beta-2B chain, neurocalcin delta, alpha-2-macroglobulin receptor-associated protein and transforming growth factor beta (TGFB1), that in turn may represent involvement of the TGFB-1 signaling cascade in neuronal development [52]. The network link between TGFB1 and Elongation factor Tu and dihydropyrimidinase-related protein 3 supports the notion that TGFB1-mediated differentiation [53], neuronal remodeling [54], neuronal cell fate [55] and neurogenesis [56] may occur in Gls knock-out

mouse brain and has to be investigated. Differentiation of brain cells that has yet to be investigated in the Gls deficient mice, but may also be affected by abnormal levels of retinol-binding protein 1 in Gls hets as the retinoic signaling cascades are involved in neuronal differentiation [57].

No specific function of the network component hepatocyte nuclear factor 4 alpha in the brain can be proposed but it is known as a multifunctional protein (https://reports.ingenuity.com/rs/nodeview.jsp?analysisid=-1&did=ING%3A86t) and the multitude of interaction partners in the current network challenge further studies into its probable roles in the Gls null mouse. Likewise, information on mutl, homolog 1 proposed as a network component, does not allow any conclusions for brain function (https://reports.ingenuity.com/rs/nodeview.jsp?analysisid=-1&did=ING%3A7zg).

Few proteomic studies have been conducted on transgenic mice during early development. The present results illustrate the broad range of compensations that arise as a result of deficiency or knockout of just one protein. Although KGA in adult brain is under considerable feedback inhibition, the genotypic reduction nonetheless leads to reduced function [58]. For some proteins, there is sufficient functional reserve so that the hets are no different than the wild types, and the alteration is only evident in the nulls. Other proteins are strikingly altered in the hets but not the nulls, suggesting that stronger compensatory changes are induced in the nulls, which appear to partially compensate for the deficiency. While many proteins are increased in potential compensation, others are down regulated. Many more proteins are likely altered in Gls deficient mice, but the present analysis is limited to the more abundant proteins.

Taken together, this gel-based proteomic approach that has to be complemented by studying additional developmental periods accompanied by partial verification of results by immunoblotting, leads to the identification of an interaction network that may contribute to the understanding and further investigation of Gls deficient mice and in the Gls hets the networks involved in engendering the SCZ resilient phenotype.

Supplementary Material

Refer to Web version on PubMed Central for supplementary material.

Acknowledgments

We acknowledge the contribution by the Verein zur Durchführung der wissenschaftlichen Forschung auf dem Gebiet der Neonatologie und Kinderintensivmedizin “Unser Kind” (GL), and support from a Columbia University Research Initiative in Science and Engineering (RISE) award and NIMH grant R01 MH087758 (SR).

References

1. Nicklas WJ, Zeevalk G, Hyndman A. Interactions between neurons and glia in glutamate/glutamine compartmentation. Biochemical Society transactions. 1987; 15:208–10. [PubMed: 2884147]
2. Kvamme E, Roberg B, Torgner IA. Phosphate-activated glutaminase and mitochondrial glutamine transport in the brain. Neurochemical research. 2000; 25:1407–19. [PubMed: 11059811]
3. Perera SY, Chen TC, Curthoys NP. Biosynthesis and processing of renal mitochondrial glutaminase in cultured proximal tubular epithelial cells and in isolated mitochondria. The Journal of biological chemistry. 1990; 265:17764–70. [PubMed: 2211660]
4. Srinivasan M, Kalousek F, Curthoys NP. In vitro characterization of the mitochondrial processing and the potential function of the 68-kDa subunit of renal glutaminase. The Journal of biological chemistry. 1995; 270:1185–90. [PubMed: 7836378]

5. Curthoys NP, Watford M. Regulation of glutaminase activity and glutamine metabolism. Annual review of nutrition. 1995; 15:133–59.
6. Elgadi KM, Meguid RA, Qian M, Souba WW, Abcouwer SF. Cloning and analysis of unique human glutaminase isoforms generated by tissue-specific alternative splicing. Physiological genomics. 1999; 1:51–62. [PubMed: 11015561]
7. Olalla L, Gutierrez A, Campos JA, Khan ZU, Alonso FJ, Segura JA, et al. Nuclear localization of L-type glutaminase in mammalian brain. The Journal of biological chemistry. 2002; 277:38939–44. [PubMed: 12163477]
8. Aledo JC, Gomez-Fabre PM, Olalla L, Marquez J. Identification of two human glutaminase loci and tissue-specific expression of the two related genes. Mammalian genome : official journal of the International Mammalian Genome Society. 2000; 11:1107–10. [PubMed: 11130979]
9. Aoki C, Kaneko T, Starr A, Pickel VM. Identification of mitochondrial and non-mitochondrial glutaminase within select neurons and glia of rat forebrain by electron microscopic immunocytochemistry. Journal of neuroscience research. 1991; 28:531–48. [PubMed: 1714509]
10. Laake JH, Slyngstad TA, Haug FM, Ottersen OP. Glutamine from glial cells is essential for the maintenance of the nerve terminal pool of glutamate: immunogold evidence from hippocampal slice cultures. Journal of neurochemistry. 1995; 65:871–81. [PubMed: 7616248]
11. Hertz L. Functional interactions between neurons and astrocytes I. Turnover and metabolism of putative amino acid transmitters. Progress in neurobiology. 1979; 13:277–323. [PubMed: 42117]
12. Hertz L, Zielke HR. Astrocytic control of glutamatergic activity: astrocytes as stars of the show. Trends in neurosciences. 2004; 27:735–43. [PubMed: 15541514]
13. Kam K, Nicoll R. Excitatory synaptic transmission persists independently of the glutamate-glutamine cycle. The Journal of neuroscience : the official journal of the Society for Neuroscience. 2007; 27:9192–200. [PubMed: 17715355]
14. Takeda K, Ishida A, Takahashi K, Ueda T. Synaptic vesicles are capable of synthesizing the VGLUT substrate glutamate from alpha-ketoglutarate for vesicular loading. Journal of neurochemistry. 2012; 121:184–96. [PubMed: 22309504]
15. Maciejewski PK, Rothman DL. Proposed cycles for functional glutamate trafficking in synaptic neurotransmission. Neurochemistry international. 2008; 52:809–25. [PubMed: 18006192]
16. Masson J, Darmon M, Conjard A, Chuhma N, Ropert N, Thoby-Brisson M, et al. Mice lacking brain/kidney phosphate-activated glutaminase have impaired glutamatergic synaptic transmission, altered breathing, disorganized goal-directed behavior and die shortly after birth. The Journal of neuroscience : the official journal of the Society for Neuroscience. 2006; 26:4660–71. [PubMed: 16641247]
17. Gaisler-Salomon I, Miller GM, Chuhma N, Lee S, Zhang H, Ghoddoussi F, et al. Glutaminase-deficient mice display hippocampal hypoactivity, insensitivity to pro-psychotic drugs and potentiated latent inhibition: relevance to schizophrenia. Neuropsychopharmacology : official publication of the American College of Neuropsychopharmacology. 2009; 34:2305–22. [PubMed: 19516252]
18. Chen W, Mahadomrongkul V, Berger UV, Bassan M, DeSilva T, Tanaka K, et al. The glutamate transporter GLT1a is expressed in excitatory axon terminals of mature hippocampal neurons. The Journal of neuroscience : the official journal of the Society for Neuroscience. 2004; 24:1136–48. [PubMed: 14762132]
19. Bleich S, Romer K, Wiltfang J, Kornhuber J. Glutamate and the glutamate receptor system: a target for drug action. International journal of geriatric psychiatry. 2003; 18:S33–40. [PubMed: 12973748]
20. Hannan AJ. Novel therapeutic targets for Huntington's disease. Expert opinion on therapeutic targets. 2005; 9:639–50. [PubMed: 16083335]
21. Schaeffer EL, Gattaz WF. Cholinergic and glutamatergic alterations beginning at the early stages of Alzheimer disease: participation of the phospholipase A2 enzyme. Psychopharmacology. 2008; 198:1–27. [PubMed: 18392810]
22. Driscoll BF, Deibler GE, Law MJ, Crane AM. Damage to neurons in culture following medium change: role of glutamine and extracellular generation of glutamate. Journal of neurochemistry. 1993; 61:1795–800. [PubMed: 7901333]

23. Choudary PV, Molnar M, Evans SJ, Tomita H, Li JZ, Vawter MP, et al. Altered cortical glutamatergic and GABAergic signal transmission with glial involvement in depression. Proceedings of the National Academy of Sciences of the United States of America. 2005; 102:15653–8. [PubMed: 16230605]
24. Bruneau EG, McCullumsmith RE, Haroutunian V, Davis KL, Meador-Woodruff JH. Increased expression of glutaminase and glutamine synthetase mRNA in the thalamus in schizophrenia. Schizophrenia research. 2005; 75:27–34. [PubMed: 15820321]
25. Gluck MR, Thomas RG, Davis KL, Haroutunian V. Implications for altered glutamate and GABA metabolism in the dorsolateral prefrontal cortex of aged schizophrenic patients. The American journal of psychiatry. 2002; 159:1165–73. [PubMed: 12091195]
26. Harrison PJ, Weinberger DR. Schizophrenia genes, gene expression, and neuropathology: on the matter of their convergence. Molecular psychiatry. 2005; 10:40–68. image 5. [PubMed: 15263907]
27. Schobel SA, Lewandowski NM, Corcoran CM, Moore H, Brown T, Malaspina D, et al. Differential targeting of the CA1 subfield of the hippocampal formation by schizophrenia and related psychotic disorders. Archives of general psychiatry. 2009; 66:938–46. [PubMed: 19736350]
28. Hoorn EJ, Hoffert JD, Knepper MA. Combined proteomics and pathways analysis of collecting duct reveals a protein regulatory network activated in vasopressin escape. Journal of the American Society of Nephrology : JASN. 2005; 16:2852–63. [PubMed: 16079266]
29. Raponi M, Belly RT, Karp JE, Lancet JE, Atkins D, Wang Y. Microarray analysis reveals genetic pathways modulated by tipifarnib in acute myeloid leukemia. BMC cancer. 2004; 4:56. [PubMed: 15329151]
30. Siripurapu V, Meth J, Kobayashi N, Hamaguchi M. DBC2 significantly influences cell-cycle, apoptosis, cytoskeleton and membrane-trafficking pathways. Journal of molecular biology. 2005; 346:83–9. [PubMed: 15663929]
31. Carr S, Aebersold R, Baldwin M, Burlingame A, Clauser K, Nesvizhskii A. The need for guidelines in publication of peptide and protein identification data: Working Group on Publication Guidelines for Peptide and Protein Identification Data. Molecular & cellular proteomics : MCP. 2004; 3:531–3. [PubMed: 15075378]
32. Tsuji A, Kikuchi Y, Sato Y, Koide S, Yuasa K, Nagahama M, et al. A proteomic approach reveals transient association of reticulocalbin-3, a novel member of the CREC family, with the precursor of subtilisin-like proprotein convertase, PACE4. The Biochemical journal. 2006; 396:51–9. [PubMed: 16433634]
33. de la Rosa V, Campos-Sandoval JA, Martin-Rufian M, Cardona C, Mates JM, Segura JA, et al. A novel glutaminase isoform in mammalian tissues. Neurochemistry international. 2009; 55:76–84. [PubMed: 19428810]
34. Mates JM, Segura JA, Campos-Sandoval JA, Lobo C, Alonso L, Alonso FJ, et al. Glutamine homeostasis and mitochondrial dynamics. The international journal of biochemistry & cell biology. 2009; 41:2051–61. [PubMed: 19703661]
35. Martin-Rufian M, Tosina M, Campos-Sandoval JA, Manzanares E, Lobo C, Segura JA, et al. Mammalian glutaminase Gls2 gene encodes two functional alternative transcripts by a surrogate promoter usage mechanism. PloS one. 2012; 7:e38380. [PubMed: 22679499]
36. Aizawa S, Sakai T, Sakata I. Glutamine and glutamic acid enhance thyroid-stimulating hormone beta subunit mRNA expression in the rat pars tuberalis. The Journal of endocrinology. 2012; 212:383–94. [PubMed: 22219301]
37. Hu W, Zhang C, Wu R, Sun Y, Levine A, Feng Z. Glutaminase 2, a novel p53 target gene regulating energy metabolism and antioxidant function. Proceedings of the National Academy of Sciences of the United States of America. 2010; 107:7455–60. [PubMed: 20378837]
38. Marquez J, Tosina M, de la Rosa V, Segura JA, Alonso FJ, Mates JM, et al. New insights into brain glutaminases: beyond their role on glutamatergic transmission. Neurochemistry international. 2009; 55:64–70. [PubMed: 19428808]
39. Erecinska M, Zaleska MM, Nelson D, Nissim I, Yudkoff M. Neuronal glutamine utilization: glutamine/glutamate homeostasis in synaptosomes. Journal of neurochemistry. 1990; 54:2057–69. [PubMed: 1971010]

40. Kvamme E, Svenneby G, Torgner IA. Calcium stimulation of glutamine hydrolysis in synaptosomes from rat brain. Neurochemical research. 1983; 8:25–38. [PubMed: 6856016]
41. Yoo BC, Fountoulakis M, Cairns N, Lubec G. Changes of voltage-dependent anion-selective channel proteins VDAC1 and VDAC2 brain levels in patients with Alzheimer's disease and Down syndrome. Electrophoresis. 2001; 22:172–9. [PubMed: 11197169]
42. Kaltenbach LS, Romero E, Becklin RR, Chettier R, Bell R, Phansalkar A, et al. Huntingtin interacting proteins are genetic modifiers of neurodegeneration. PLoS genetics. 2007; 3:e82. [PubMed: 17500595]
43. Culver BP, Savas JN, Park SK, Choi JH, Zheng S, Zeitlin SO, et al. Proteomic analysis of wild-type and mutant huntingtin-associated proteins in mouse brains identifies unique interactions and involvement in protein synthesis. The Journal of biological chemistry. 2012; 287:21599–614. [PubMed: 22556411]
44. Lei G, Xia Y, Johnson KM. The role of Akt-GSK-3beta signaling and synaptic strength in phencyclidine-induced neurodegeneration. Neuropsychopharmacology : official publication of the American College of Neuropsychopharmacology. 2008; 33:1343–53. [PubMed: 17637606]
45. Wang Q, Liu L, Pei L, Ju W, Ahmadian G, Lu J, et al. Control of synaptic strength, a novel function of Akt. Neuron. 2003; 38:915–28. [PubMed: 12818177]
46. Pratt KG, Zimmerman EC, Cook DG, Sullivan JM. Presenilin 1 regulates homeostatic synaptic scaling through Akt signaling. Nature neuroscience. 2011; 14:1112–4.
47. Majumdar D, Nebhan CA, Hu L, Anderson B, Webb DJ. An APPL1/Akt signaling complex regulates dendritic spine and synapse formation in hippocampal neurons. Molecular and cellular neurosciences. 2011; 46:633–44. [PubMed: 21236345]
48. Horwood JM, Dufour F, Laroche S, Davis S. Signalling mechanisms mediated by the phosphoinositide 3-kinase/Akt cascade in synaptic plasticity and memory in the rat. The European journal of neuroscience. 2006; 23:3375–84. [PubMed: 16820027]
49. Bruel-Jungerman E, Veyrac A, Dufour F, Horwood J, Laroche S, Davis S. Inhibition of PI3K-Akt signaling blocks exercise-mediated enhancement of adult neurogenesis and synaptic plasticity in the dentate gyrus. PloS one. 2009; 4:e7901. [PubMed: 19936256]
50. Beaulieu JM, Sotnikova TD, Marion S, Lefkowitz RJ, Gainetdinov RR, Caron MG. An Akt/beta-arrestin 2/PP2A signaling complex mediates dopaminergic neurotransmission and behavior. Cell. 2005; 122:261–73. [PubMed: 16051150]
51. Hou L, Klann E. Activation of the phosphoinositide 3-kinase-Akt-mammalian target of rapamycin signaling pathway is required for metabotropic glutamate receptor-dependent long-term depression. The Journal of neuroscience : the official journal of the Society for Neuroscience. 2004; 24:6352–61. [PubMed: 15254091]
52. Yun C, Mendelson J, Blake T, Mishra L, Mishra B. TGF-beta signaling in neuronal stem cells. Disease markers. 2008; 24:251–5. [PubMed: 18525119]
53. Yi JJ, Barnes AP, Hand R, Polleux F, Ehlers MD. TGF-beta signaling specifies axons during brain development. Cell. 2010; 142:144–57. [PubMed: 20603020]
54. Awasaki T, Huang Y, O'Connor MB, Lee T. Glia instruct developmental neuronal remodeling through TGF-beta signaling. Nature neuroscience. 2011; 14:821–3.
55. Vogel T, Ahrens S, Buttner N, Krieglstein K. Transforming growth factor beta promotes neuronal cell fate of mouse cortical and hippocampal progenitors in vitro and in vivo: identification of Nedd9 as an essential signaling component. Cereb Cortex. 2010; 20:661–71. [PubMed: 19587023]
56. Misumi S, Kim TS, Jung CG, Masuda T, Urakawa S, Isobe Y, et al. Enhanced neurogenesis from neural progenitor cells with G1/S-phase cell cycle arrest is mediated by transforming growth factor beta1. The European journal of neuroscience. 2008; 28:1049–59. [PubMed: 18783370]
57. Toresson H, Mata de Urquiza A, Fagerstrom C, Perlmann T, Campbell K. Retinoids are produced by glia in the lateral ganglionic eminence and regulate striatal neuron differentiation. Development. 1999; 126:1317–26. [PubMed: 10021349]
58. El Hage M, Masson J, Conjard-Duplany A, Ferrier B, Baverel G, Martin G. Brain slices from glutaminase-deficient mice metabolize less glutamine: a cellular metabolomic study with carbon 13 NMR. Journal of cerebral blood flow and metabolism : official journal of the International Society of Cerebral Blood Flow and Metabolism. 2012; 32:816–2. [PubMed: 22373647]

Abbreviations

ACN	Acetonitrile
CHAPS	3-[(3-cholamidopropyl)dimethylamonio]-1-propanesulphonate
GABA	γ-aminobutyric acid
Gln	Glutamine
Glu	Glutamate
IPA	Ingenuity Pathway Analysis
KGA	Kidney-type glutaminase
LGA	Liver-type glutaminase
OGP	Octyl β-D-glucopyranoside
PMSF	phenylmethylsulphonyl fluoride
PVDF	polyvinylidene difluoride
SCZ	Schizophreina
TBST	Tris-Buffered Saline and Tween 20

Highlights

- The network of glutaminase-dependent brain proteins was identified by LC-MS/MS.
- Fetal glutaminase deficiency affected network involved in cellular assembly.
- Fetal glutaminase deficiency linked to neuropathology
- Glutaminase plays important roles in brain cell maturation.

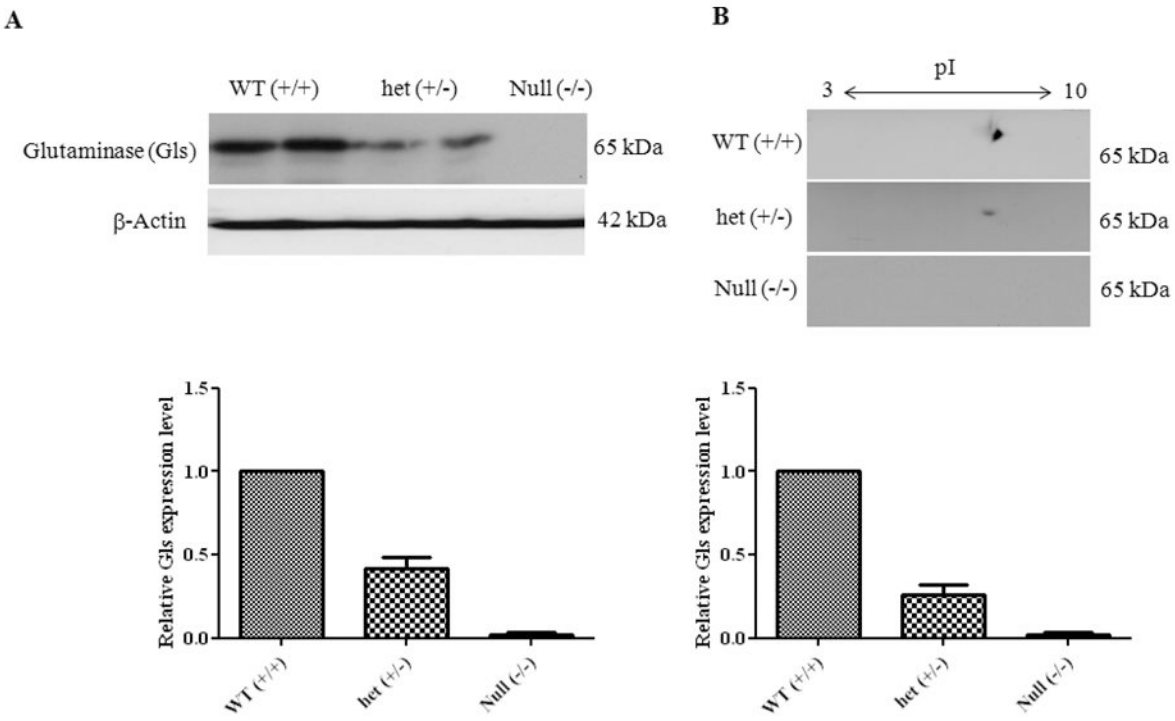

Figure 1.

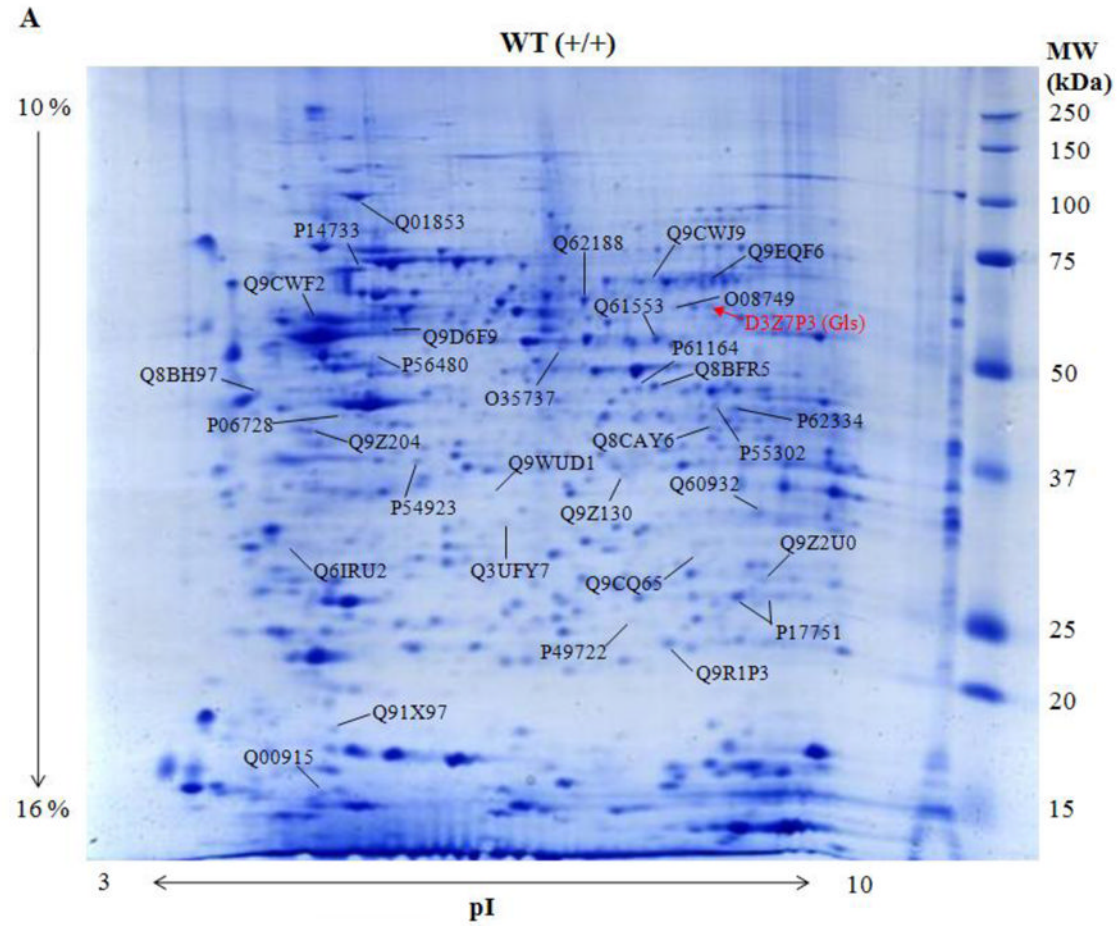

Figure 2A

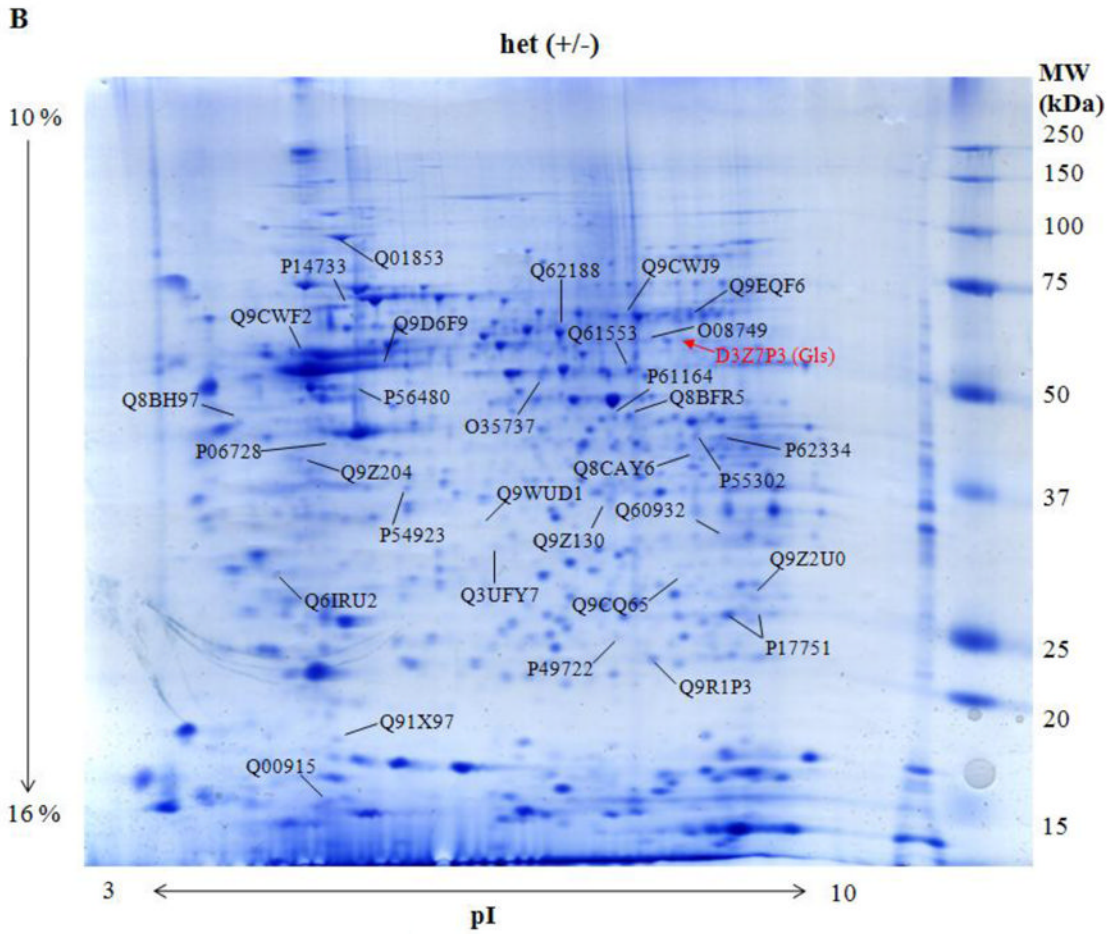

Figure 2B

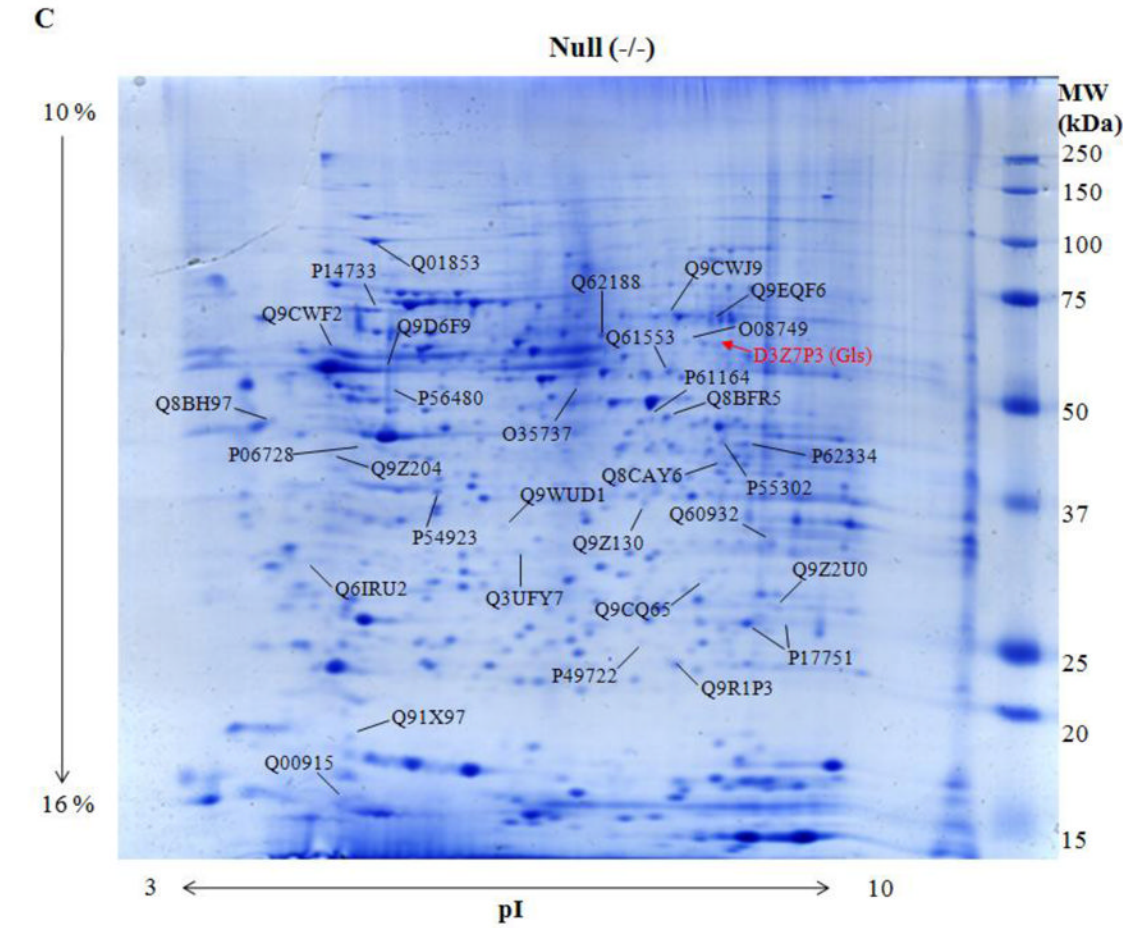

Figure 2C

Figure 2.

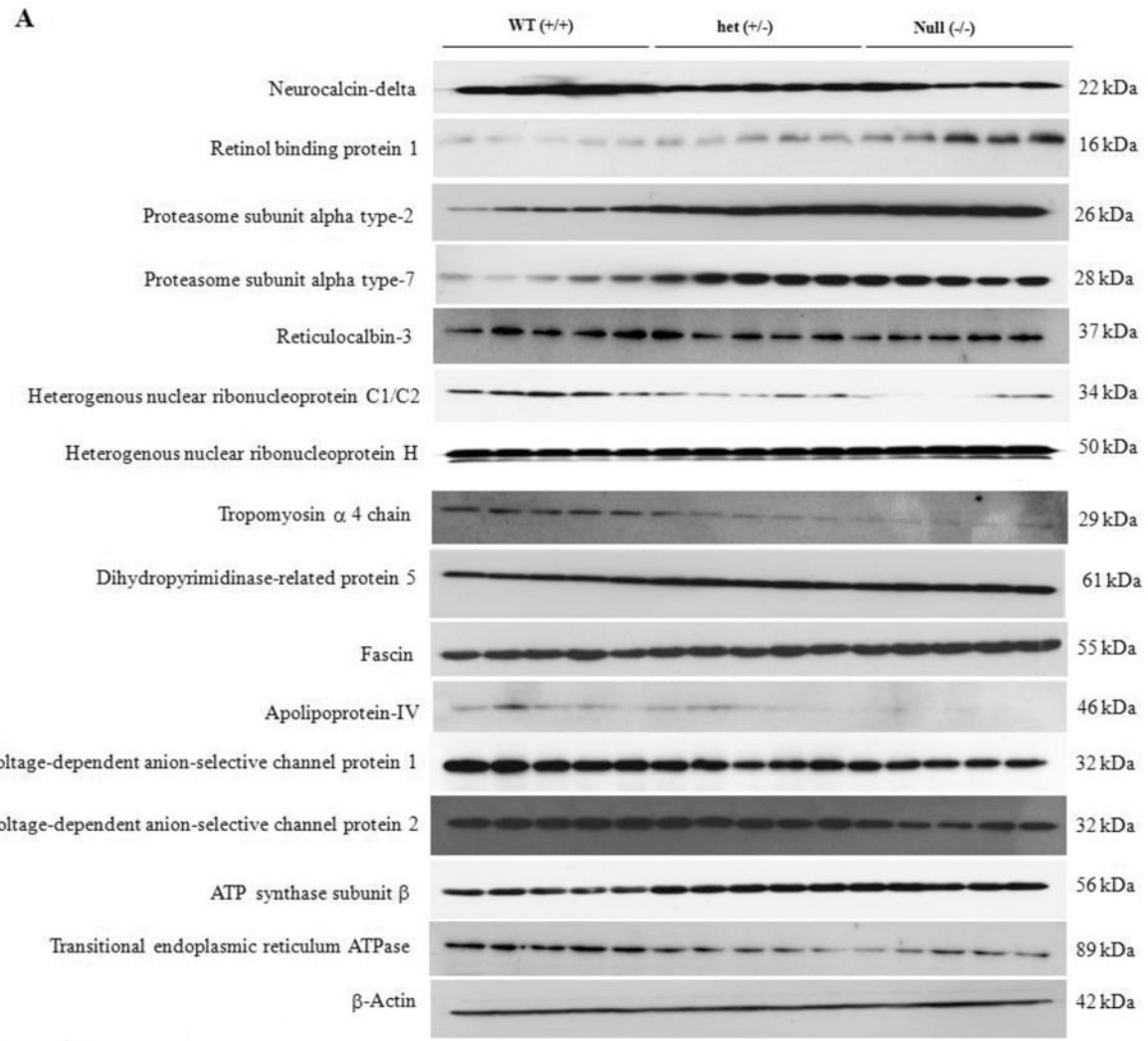

Figure 3A

B

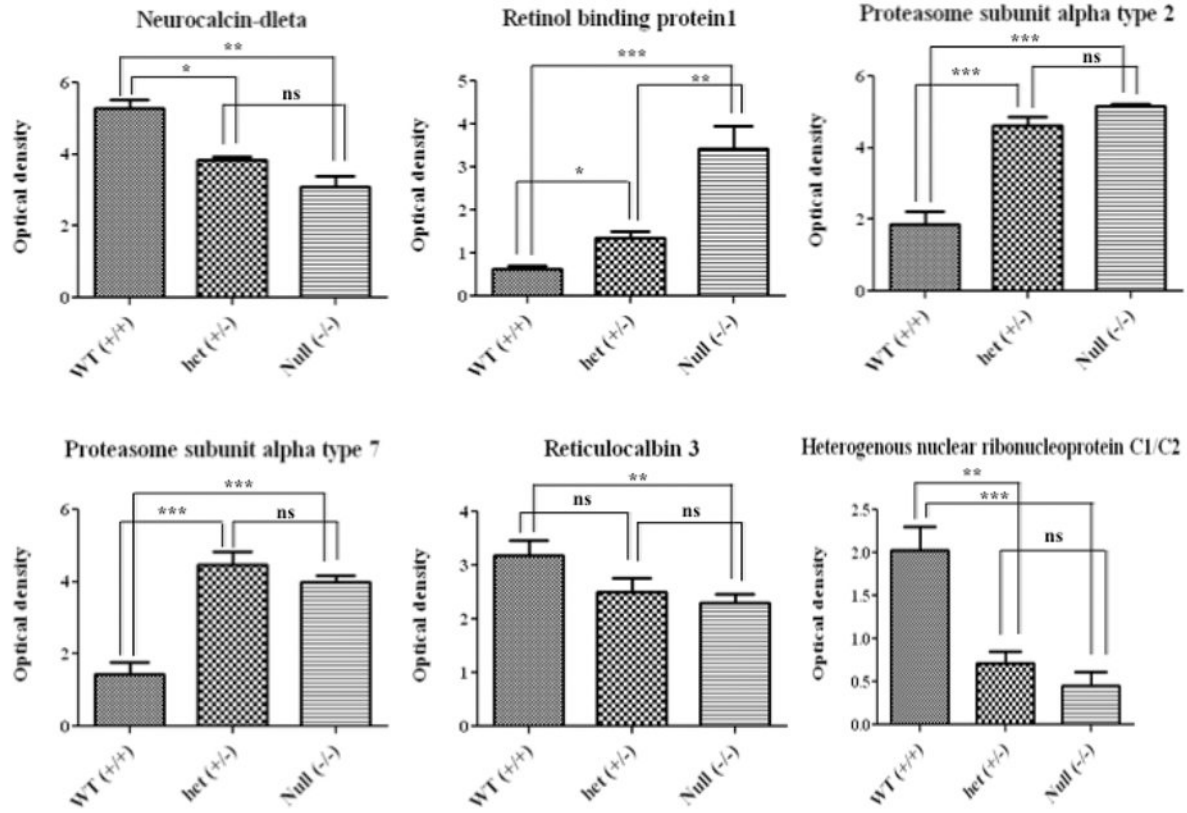

Figure 3B-1

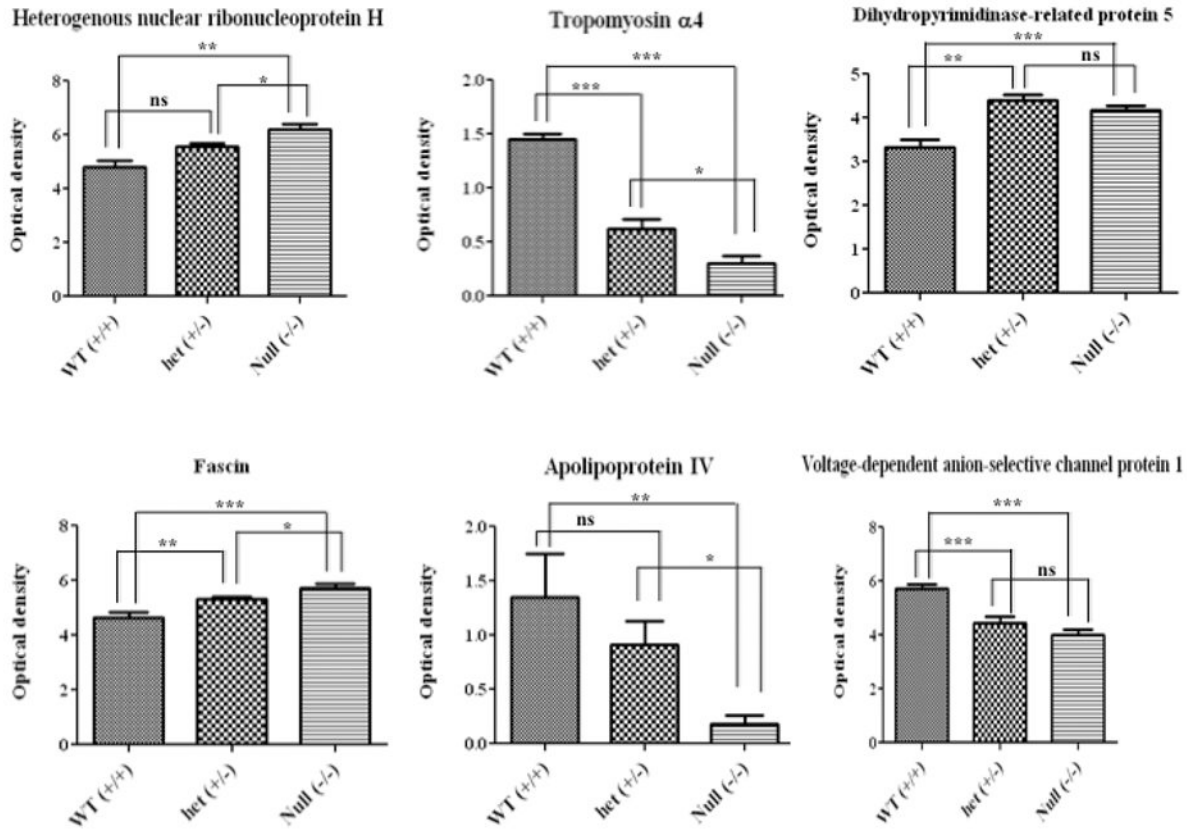

Figure 3B-2

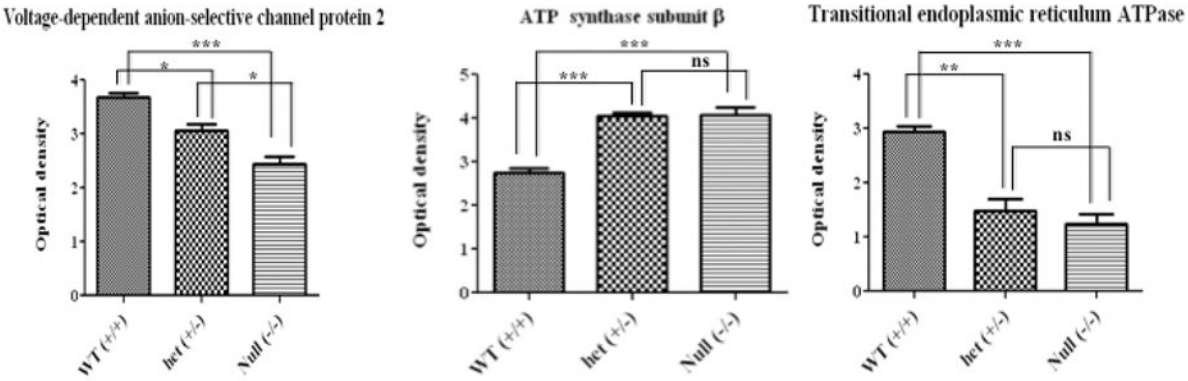

Figure 3B-3

Figure 3.

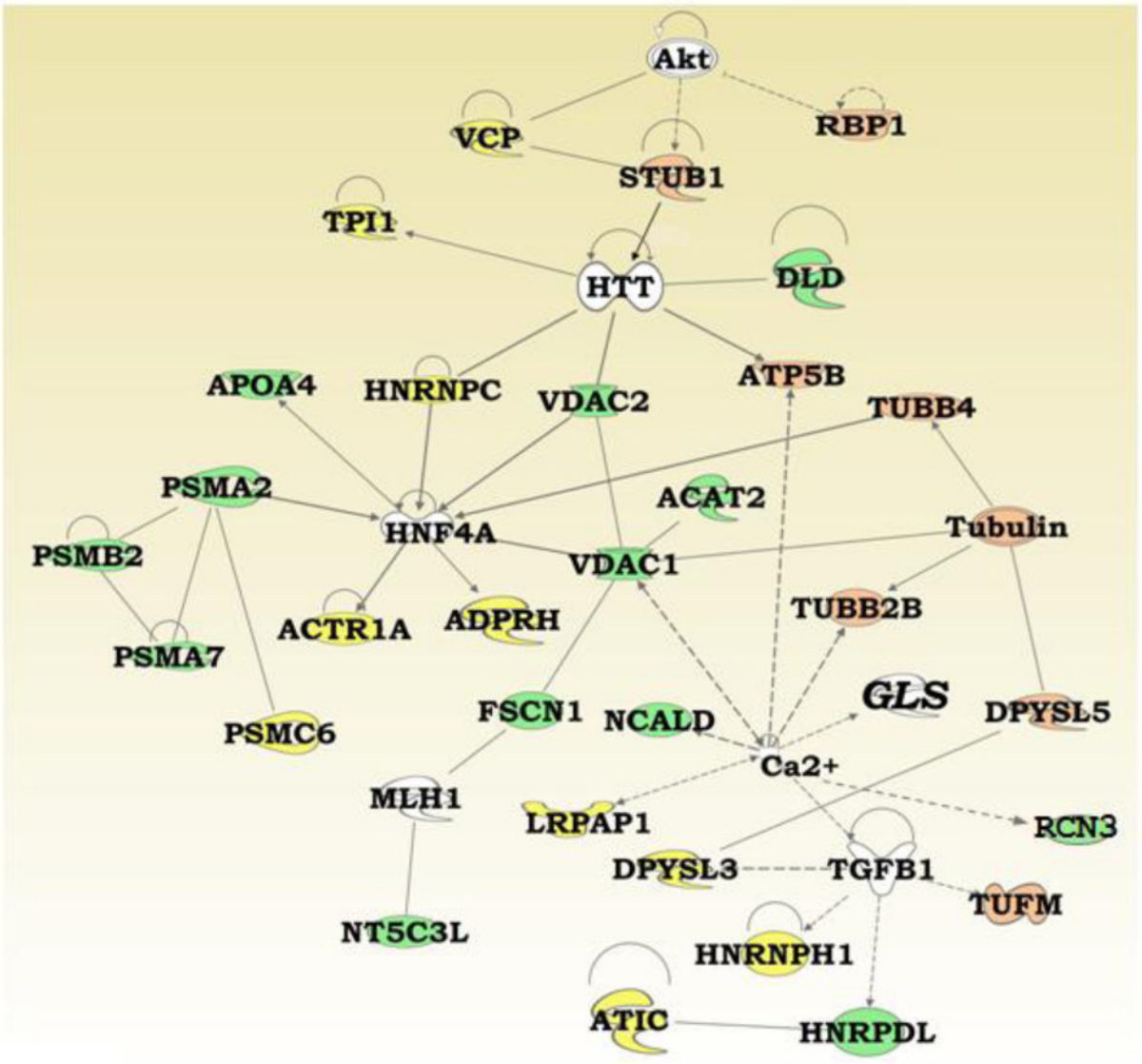

Figure 4.

Table 1
Primary antibodies used for Western blotting

Protein name	Species	MW (kDa)	Dilution	Manufacturer (catalog number)
Glutaminase	Rabbit	65	1:5000	Abcam (ab93434)
Neurocalcin delta	Rabbit	22	1:5000	Abcam (ab107977)
Retinol binding protein 1	Rabbit	16	1:3000	Acris Antibodies GmbH (AP16335PU-N)
Proteasome subunit alpha type 2	Rabbit	26	1:5000	Genetex (GTX63160)
Proteasome subunit alpha type 7	Rabbit	28	1:5000	Genetex (GTX113531)
Reticulocalbin 3	Goat	37	1:3000	Santa Cruz (sc-162090)
Heterogenous nuclear rebonucleoprotein C1/C2	Rabbit	34	1:5000	Acris Antibodies GmbH (AP20405PU-N)
Heterogenous nuclear rebonucleoprotein H	Rabbit	50	1:3000	Abcam (ab10374)
Tropomyosin alpha 4	Rabbit	29	1:3000	Proteintech Group (13741-1-AP)
Fascin	Rabbit	55	1:3000	Abcam (ab78487)
Dihydropyriminidase-related protein 5	Rabbit	61	1:5000	Proteintech Group (10525-1-AP)
Apolipoprotein-IV	Rabbit	46	1:1000	Santa Cruz (sc-50376)
Volatage dependent anion selective channel protein 1	Goat	32	1:5000	Santa Cruz (sc-32063)
Volatage dependent anion selective channel protein 2	Goat	32	1:5000	Santa Cruz (sc-32059)
ATP synthease subunit beta	Mouse	56	1:3000	Abcam (ab5432)
Transitional endoplasmic reticulum ATPase	Rabbit	89	1:5000	Acris Antibodies GmbH (AP21142PU-N)
Actin (loading control)	Rabbit	42	1:5000	Abcam (ab1801)

Table 2

Protein quantification results of significantly changed spots on 2DE (n=33)

		Mean ± SD			p[a]	*Post hoc*			Fold chang e[b]	
Spot no.	**Protein name (Accession no.)**	**WT (+/+)**	**het (+/-)**	**Null (-/-)**		**WT vs het**	**WT vs null**	**het vs null**	**het**	**Null**
1. Significantly changed levels of spots in Gls het brain (n=9)										
19	Retinol-binding protein 1 (Q00915)	13951.90 ± 5839.56	34331.03 ± 8046.42	22144.89 ± 7546.81	*	**0.035**	0.102	**0.047**	2.46	1.59
109	S-methyl-5′-thioadenosine phosphorylase (Q9CQ65)	6265.68 ± 3540.64	18939.68 ± 10232.67	9103.90 ± 6772. 40	**	**0.004**	0.373	**0.019**	3.02	1.45
156	STIP1 homology and U box-containing protein 1 (Q9WUD1)	5992.28 ± 2314.32	3941.94 ± 1235.27	2428.28 ± 1236.24	*	**0.036**	0.097	0.330	0.66	0.41
234	Elongation factor Tu, mitochondrial (Q8BFR5)	12037.00 ± 4762.086	6065.88 ± 3149.35	6271.44 ± 3007.26	*	**0.045**	0.069	0.377	0.50	0.52
282	Tubulin beta-2B chain (Q9CWF2)	118442.22 ± 88624.17	36820.54 ± 17482.46	38643.98 ± 32621.24	*	**0.047**	0.066	0.701	0.31	0.33
287	Tubulin beta-4 chain (Q9D6F9)	61195.35 ± 19842.35	144989.65 ± 38252.55	158188.84 ± 52792.44	*	**0.032**	0.159	0.120	2.37	2.58
288	ATP synthase subunit beta, mitochondrial (P56480)	8821.13 ± 6015.60	72338.81 ± 16565.68	34712.30 ± 1331.98	*	**0.027**	0.470	0.120	8.02	3.94
302	Lamin-B1 (P14733)	52767.93 ± 6396.73	43988.29 ± 16064.52	41966.31 ± 7571.82	**	**0.006**	0.291	**0.013**	0.83	0.80
373	Dihydropyrimidinase-related protein 5 (Q9EQF6)	28992.85 ± 8020.66	61812.92 ± 14468.39	47618.75 ± 5767.81	**	**0.003**	0.067	0.232	2.13	1.64
2. Significantly changed levels of spots in Gls null brain (n=10)										
98	Triosephosphate isomerase (P17751)	70569.48 ± 12649.70	79792.91 ± 10297.80	100700.96 ± 19984.44	**	0.053	**0.005**	**0.042**	1.13	1.43
102	Triosephosphate isomerase (P17751)	13731.34 ± 5074.16	20767.88 ± 8540.68	40859.43 ± 6162.35	**	0.095	**0.004**	**0.048**	1.51	2.98
149	[Protein ADP-ribosylarginine] hydrolase (P54923)	39430.68 ± 7698.19	30079.50 ±8806.57	16037.75 ± 5206.40	**	0.168	**0.011**	**0.008**	0.76	0.41
171	Heterogeneous nuclear ribonucleoproteins C1/C2 (Q9Z204)	28496.09 ± 10382.64	27061.08 ± 7716.76	8015.51 ± 8537.85	**	0.086	**0.011**	**0.008**	0.95	0.28
225	Alpha-2-macroglobulin receptor-associated protein (P55302)	24923.50 ± 6631.08	13958.55 ± 10401.01	13887.34 ± 10575.18	*	0.053	**0.045**	0.491	0.56	0.56
226	26S protease regulatory subunit 10B (P62334)	24365.11 ± 5028.49	35095.46 ± 6248.21	35591.20 ± 3887.54	*	0.055	**0.038**	0.546	1.44	1.46
240	Alpha-centractin (P61164)	24758.53 ± 8070.90	20283.39 ± 5538.27	15638.64 ± 4849.33	*	0.275	**0.029**	0.261	0.82	0.63
334	Dihydropyrimidinase-related protein 3 (Q62188)	61785.76 ± 8949.37	66029.06 ± 9688.29	79849.23 ± 6721.76	**	0.144	**0.008**	0.018	1.07	1.29
350	Heterogeneous nuclear ribonucleoprotein H (O35737)	17001.97 ± 2720.86	18598.58 ± 1763.45	27307.31 ± 3980.99	**	0.523	**0.003**	**0.027**	1.09	1.61
370	Bifunctional purine biosynthesis protein PURH (Q9CWJ9)	27531.33 ± 9866.91	28206.4 ± 5636.48	7089.65 ± 3580.55	**	0.545	**0.008**	**0.007**	1.02	0.26
392	Transitional endoplasmic reticulum ATPase (Q01853)	101399.30 ± 15315.96	78972.69 ± 11576.30	50031.86 ± 13094.12	**	0.150	**0.005**	**0.042**	0.78	0.49
3. Significantly changed levels of spots in both Gls het and Gls null brain(n=13)										

		Mean ± SD			p[a]	Post hoc			Fold chang e[b]	
Spot no.	**Protein name (Accession no.)**	**WT (+/+)**	**het (+/-)**	**Null (-/-)**		**WT vs het**	**WT vs null**	**het vs null**	**het**	**Null**
6	Neurocalcin-delta (Q91X97)	24045.40 ± 4323.41	8412.26 ± 3992.18	7478.05 ± 1542.34	**	**0.007**	**0.025**	**0.011**	0.35	0.31
92	Proteasome subunit alpha type-2 (P49772)	9087.09 ± 2670.75	18449.95 ± 5035.35	17218.40 ± 6113.19	**	**0.006**	**0.005**	0.570	2.03	1.89
93	Proteasome subunit beta type-2 (Q9R1P3)	26265.03 ± 4712.83	41121.89 ± 5070.36	37184.91 ± 3411.54	**	**0.008**	**0.028**	0.290	1.57	1.42
108	Proteasome subunit alpha type-7 (Q9Z2U0)	6488.74 ± 2837.29	16524.84 ± 2560.06	18256 ± 3024.42	**	**0.020**	**0.005**	0.368	2.55	2.81
116(1)[c]	Voltage-dependent anion-selective channel protein 1 (Q60932)	40718.60 ± 8595.87	26756.10 ± 8653.23	17953.48 ± 8621.31	**	**0.016**	**0.007**	0.146	0.66	0.44
116(2)[c]	Voltage-dependent anion-selective channel protein 2(Q60932)									
135	Cytosolic 5'-nucleotidase III-like protein (Q3UFY7)	13719.58 ± 4721.60	8962.79 ± 1933.32	6661.58 ± 3664.56	*	**0.035**	**0.049**	0.331	0.65	0.49
175	Reticulocalbin-3 (Q8BH97)	23967.86 ± 3930.57	13500.35 ± 4913.81	11800.88 ± 4266.58	**	**0.003**	**0.012**	0.501	0.56	0.49
181	Apolipoprotein A-4(P06728)	12924.66 ± 5308.90	4216.12 ± 2649.09	7371.28 ± 3551.27	*	**0.023**	**0.036**	0.274	0.33	0.57
194	Heterogeneous nuclear ribonucleoprotein D-like (Q9Z130)	42348.95 ± 7125.00	31005.96 ± 6646.84	23005.76 ± 1930.87	**	**0.017**	**0.006**	0.096	0.73	0.54
224	Acetyl-CoA acetyltransferase, cytosolic (Q8CAY6)	17844.71 ± 4985.94	8574.85 ± 2933.88	5754.76 ± 1945.68	**	**0.027**	**0.004**	0.277	0.48	0.32
354	Fascin (Q61553)	40661.85 ± 5533.86	61080.50 ± 6746.64	52211.54 ± 6614.30	**	**0.003**	**0.014**	0.112	1.5	1.28
359	Dihydrolipoyl dehydrogenase, mitochondrial (O08749)	11621.07 ± 2228.26	9003.81 ± 1029.75	6527.38 ± 1847.74	**	**0.031**	**0.006**	0.126	0.77	0.56
4. Significantly changed levels of spot in Gls het vs. Gls null (n=1, not included in pathway analysis)										
122	Tropomyosin alpha-4 chain (Q6IRU2)	4966.7 ± 2218.17	4875.21 ± 1026.04	2589.71 ± 1413.15	*	0.645	0.059	**0.035**	0.98	0.52

Values with a p-value less than 0.05 are marked **in bold**

[a] ANOVA P-Value;

* P<0.05,

** P<0.01

[b] Fold change (WT vs. het or null)

[c] MASCOT protein hit list 1 and 2 of spot 116

Table 3

Abbreviation in IPA network

Abbreviation	Protein name
ACAT2	Acetyl-CoA acetyltransferase, cytosolic
ACTR1A	Alpha-centractin
ADPRH	[Protein ADP-ribosylarginine] hydrolase
Akt	Serine/threonine-proteinkinase akt
APOA4	Apolipoprotein A-IV
ATIC	Bifunctional purine biosynthesis protein PURH
ATP5B	ATP synthase subunit beta, mitochondrial
DLD	Probable D-lactate dehydrogenase, mitochondrial
DPYSL3	Dihydropyrimidinase-related protein 3
DPYSL5	Dihydropyrimidinase-related protein 5
FSCN1	Fascin
GLS	Glutaminase kidney isoform, mitochondrial
HNF4A	Hepatocyte nuclear factor 4-alpha
HNRNPC	Heterogeneous nuclear ribonucleoproteins C1/C2
HNRNPH1	Heterogeneous nuclear ribonucleoprotein H
HNRPDL	Heterogeneous nuclear ribonucleoprotein D-like
HTT	Huntingtin
LRPAP1	Alpha-2-macroglobulin receptor-associated protein
MLH1	DNA mismatch repair protein MLH1
NCALD	Neurocalcin-delta
NT5C3L	Cytosolic 5'-nucleotidase III-like protein
PSMA2	Proteasome subunit alpha 2
PSMA7	Proteasome subunit alpha type-7
PSMB2	Proteasome subunit beta 2
PSMC6	26S protease regulatory subunit 10B
RBP1	Retinol Binding potein 1
RCN3	Reticuylocalbin 3
STUB1	STIP1 homology and U box-containing protein 1
TGFB1	Transforming growth factor beta-1
TPI1	Triosephosphate isomerase
TUBB2B	Tubulin beta-2 chain
TUBB4	Tubulin beta-4 chain
TUFM	Elongation factor Tu, mitochondrial
VCP	Transitional endoplasmic reticulum ATPase
VDAC1	Voltage-dependent anion-selective channel protein 1
VDAC2	Voltage-dependent anion-selective channel protein 2